Synthesis and Properties of Crosslinked Chiral Nanoparticles via RAFT Miniemulsion Polymerization

WENLIANG XU, ZHENPING CHENG, LIFEN ZHANG, ZHENGBIAO ZHANG, JIAN ZHU, NIANCHEN ZHOU, XIULIN ZHU

Key Laboratory of Organic Synthesis of Jiangsu Province, College of Chemistry, Chemical Engineering and Materials Science, Soochow University, Suzhou 215123, China

Received 13 August 2009; accepted 13 December 2009
DOI: 10.1002/pola.23893
Published online in Wiley InterScience (www.interscience.wiley.com).

ABSTRACT: Crosslinked chiral nanoparticles were successfully synthesized via reversible addition-fragmentation chain transfer (RAFT) miniemulsion polymerization of 6-*O*-*p*-vinylbenzyl-1,2:3,4-di-*O*-isopropylidene-D-galactopyranose (VBPG) using linear poly(VBPG) as the macro-RAFT agent. The polymerization of VBPG in the absence of crosslinker was first studied and the kinetic results showed that the molecular weights of the obtained poly(VBPG) increased linearly with the monomer conversion and was in good consistency with the corresponding theoretical ones while there remained a relative narrow polydispersity. The effect of the amount of crosslinker, divinylbenzene, on the nanoparticle size and chiral separation properties of the obtained nanoparticles were investigated in detail using four racemates ±-3-Amino-1,2-propanediol, D,L-arabinose, D,L-tartaric acid, and D,L-mandelic acid. © 2010 Wiley Periodicals, Inc. J Polym Sci Part A: Polym Chem 48: 1324–1331, 2010

KEYWORDS: chiral separation; emulsion polymerization; macro-RAFT agent; nanoparticles; reversible addition-fragmentation chain transfer (RAFT)

INTRODUCTION Driven by the increasing demand for optically pure enantiomers in the chemical industry,[1,2] the interest in developing new and efficient methods to produce enantiomerically pure compounds is critical for the development of new materials, particularly pharmaceuticals, agrochemicals, and flavors.[3] Generally, chiral compounds are prepared either by asymmetric catalysis or by the chiral resolution of the enantiomers using various separation methods. Despite impressive advances in stereoselective synthesis, separation of racemic mixtures still is the most widely used method of producing single enantiomers in industry. Noteworthy systematic research of chiral separation techniques includes various chromatographic methods, such as gas chromatograph (GC), supercritical fluid chromatography (SFC), and high performance liquid chromatography (HPLC).[4–6] The HPLC method, the most popular among chromatography, mainly utilizes chiral stationary phases (CSPs) to carry out the determinations. Excellent works have been done by Okamoto et al. in this field. They developed and applied the polysaccharide-based CSPs as well as chiral packing materials (CPMs) based on optically active polymers for efficient separation of enantiomers.[7–9] It is noted that publications covering preparative chiral polymer for separation have continued to increase in recent years, which solved the problem of labor and energy intensive of chromatographic methods. Schlenoff's group reported optically active polyelectrolyte multilayers as membranes for chiral separations.[1] Goto et al. extended supported liquid membranes for chiral separation.[10] Subsequently, Zharov and coworkers developed chiral permselectivity in surface-modified nanoporous opal films for chiral separation.[11] All the aforementioned separation processes are due to enantioselective adsorption on the substrate surfaces, as reported by Gellman[12] and Ernst.[13]

Over the past decade, the controlled/"living" radical polymerization (CRP) has been demonstrated to be a potentially useful and important new approach for producing polymers with previously unattainable complex architectures in a controlled manner.[14–16] The CRP is usually conducted in a homophase system. Compared with polymerization processes in organic solvents polymerization conducted in environmentally friendly solvent such as water is the best alternative to obtain polymeric nanoparticles in large-scale providing excellent heat transfer, ease of mixing, process flexibility, and ease of handling/transporting the final latex. There are several heterophase processes that allow the formation of nanoparticles in water, for example, emulsion, miniemulsion, precipitation, suspension polymerizations, and so forth.[17,18] The well-known method of miniemulsion polymerization process is a very versatile technique for the formation of a broad range of polymers and structured materials in confined geometries. In general, miniemulsion consists of small, stable, and narrowly distributed droplets in a continuous phase. The high stability of the droplets is ensured by the combination of the surfactant, and the costabilizer, which is soluble and homogeneously distributed in the droplet phase. Such small droplets can then act as nanocontainers in which reactions can take place, either inside the droplets or at the interface of the droplets, resulting in most of the cases in forming nanoparticles. However, this system has not been

Correspondence to: X. Zhu (E-mail: xlzhu@suda.edu.cn)

particularly successful due to issues of mass transfer of the molecular weight control agent. Schork et al. have shown theoretically and experimentally that oligomers are very effective swelling agents and can cause high swelling of polymer particles with monomer, whereas polymers with high molecular weight are much less effective swelling agents.[19] Phase separation may occur in the resultant particles, possibly resulting in nonspherical particles and coagulation. Hence, macro-RAFT agent, suitable stabilizer, and costabilizer are the best choice to solve these disadvantages.[20]

Sugars are naturally occurring molecules. Derivatives of sugars, especially their oligomers and polymers as well as their bioconjugates and modifications, are everywhere in the living systems and particularly abundant on the nanoparticle surfaces. To date, many synthetic glycopolymers have been synthesized via CRP techniques. For example, Yaacoub and coworkers used RAFT miniemulsion polymerization to prepare well-defined polymers carrying saccharide moieties.[21] Lowe et al. used the same technique to polymerize monomers carrying unprotected saccharide residues,[22] due in part to their biomimetic properties.[23] Large amounts of carbohydrates are commercially available and a substantial part of the surplus of their agricultural production may be spent in this way.[24]

Chiral recognition has already been established in respect to the interactions of sugars (glucose, mannose, arabinose, and xylose) with chiral Pt single crystal surfaces,[25] where electro-oxidation accompanied adsorption and was the means whereby the enantomeric response was identified. Enlarging the availability of specific chiral surface area can enhance the efficiency of chiral separation. From practical and energetically efficient standpoint, separation of enantiomers through chiral nanoparticales will be an attractive process to carry on separation at a large scale.

Our previous work demonstrated that the linear chiral poly(6-*O*-*p*-vinylbenzyl-1,2:3,4-di-*O*-isopropylidene-D-galactopyranose) [poly(VBPG)] could be obtained by the RAFT polymerization of the monomer, VBPG in solution, and had the ability of enantioselective separation.[26] As for particles used for the enantioselective recognition, there have been some reports prepared by imprinting techniques. For example, Nilssons' group firstly prepared molecularly imprinted polymer (MIP) microparticles by precipitation polymerization, then used for enantiomer separations by a partial filling technique.[27] Quaglia et al. developed a macroporous silica particles surface-initiated polymerization technique for the preparation of MIP-based CSPs.[28] In this work, the well-defined glycopolymers and chiral nanoparticles with crosslinked structure were directly synthesized via RAFT miniemulsion technique, using chiral VBPG as the monomer and poly(VBPG) as the macro-RAFT agent. Furthermore, different chiral molecules have been used to test the ability of enantioselective recognition of the chiral nanoparticles by checking out the specific rotation of ethanol solution of the enantioselective separation.

EXPERIMENTAL

Materials

RAFT agent benzyl dithiobenzoate (BDB) and the monomer VBPG (the chemical structure is shown in Scheme 1) were synthesized as reported elsewhere.[26] Divinylbenzene (DVB) (50%, mixture of isomers, Shanghai Chemical Reagent Co.) was purified by passing it through the silica gel column. 2,2′-Azobisisobutyronitrile (AIBN, 99%, from Shanghai Chemical Reagent, China) was recrystallized twice from ethanol and dried in vacuum at room temperature overnight. Tetrahydrofuran (THF) and toluene (analytical reagent, from Shanghai Chemical Reagent Co., China) was purified by distilling in the presence of molecular sieves. Hexadecane (HD, Sigma-Aldrich, 99%), sodium dodecyl benzene sulfonate (SDS), ethanol, D,L-tartaric acid, D-(−)-mandelic acid, L-(+)-mandelic acid, D-(−)-tartaric acid, L-(+)-tartaric acid, and D,L-mandelic acid (analytical reagent, from Shanghai Chemical Reagent, China), D,L-arabinose and ± 3-amino-1,2-propanediol (Alfa Aesar, 97%), and (R)-3-amino-1,2-propanediol, (S)-3-amino-1,2-propanediol (TCI, 99%), D-(−)-arabinose and L-(+)-arabinose (Alfa Aesar, 99%) were used without further purification. In all miniemulsion experiments, deionized water (ultrapure water from Direct-Q 3 UV^{TM} Millipore) was used as a reaction medium. All other solvents and reagents were purchased from commercial sources and were used as received.

^{1}H NMR for BDB ($CDCl_3$, 400 MHz, d): 4.60 (s, 2H, CH_2—Ph), 7.30–7.60 (m, 8H, ArH), 8.02 (m, 2H, ArH).

Characterization

The mean particle sizes and size distributions of the polymer latexes were determined with a HPP 5001 high-performance particle size (HPPS) instrument (Malvern) at wavelength of 532 nm at 25 ± 0.1 °C and dynamic light scattering (DLS) on a Zetasizer Nano-ZS (Malvern Instrument) at wavelength of 633 nm at 25 ± 0.1 °C. Before the measurements, the original latex samples were diluted with deionized water to adjust the light strength suitable to the measurement condition. The cumulant method was chosen for measuring the z-average hydrodynamic diameter (D_z) and size polydispersity (denoted size PDI) were automatically analyzed in the cumulant mode by the Malvern Zetasizer software and were reported as the average of three measurements. The morphology of latex particles was studied by means of transmission electron microscopy (TEM, Tecnai, G2-20, FEI Company) with electron microscope operating at 100 kV. The diluted colloidal solutions were applied to a 400-mesh carbon-coated copper grid and left to dry for 1 day by air at room temperature before measurement. The number-average molecular weight (M_n) and molecular weight distribution (M_w/M_n) of the resulting polymers were determined using a Waters 1515 gel permeation chromatograph (GPC) equipped with a refractive index detector (Waters 2414), using HR 1 (pore size: 100 Å , 100–5000 Da), HR 2 (pore size: 500 Å, 500–20,000 Da), and HR 4 (pore size 10,000 Å, 50–100,000 Da) columns (7.8 × 300 mm^2, 5 μm beads size) with molecular weights ranging from 10^2–5 × 10^5 g/mol. Tetrahydrofuran (THF) was used as the eluent at a flow rate of 1.0 mL/min and 30 °C. The GPC samples were injected using a Waters 717 plus autosampler and calibrated with PS standards from Waters. The specific rotations were measured on an Autopol IV instrument with $\lambda = 589$ nm at 20 °C. The ^{1}H

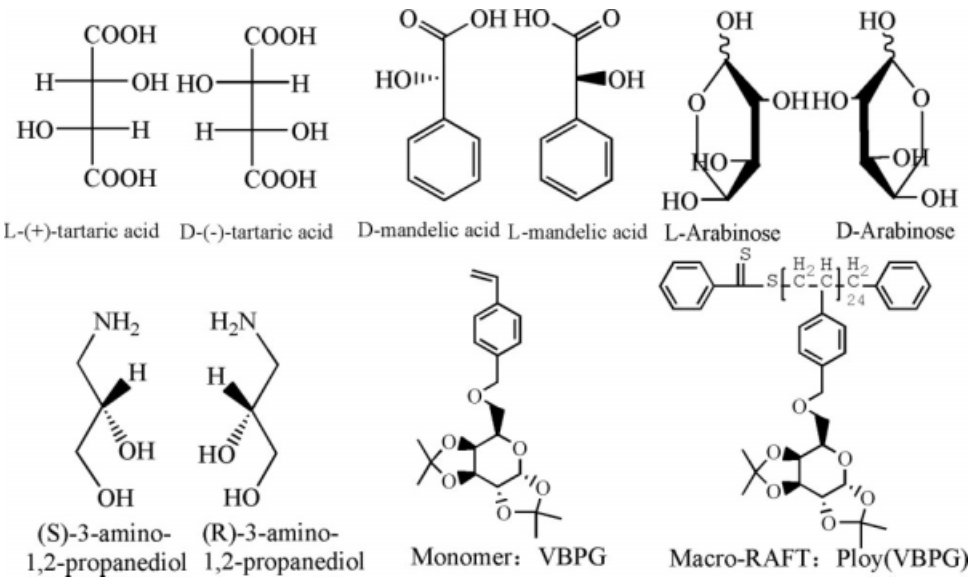

SCHEME 1 Schematic diagram illustrating the structures of racemates: D,L-tartaric acid, D,L-mandelic acid, D,L-arabinose, and ±-3-amino-1,2-propanediol; the monomer VBPG and Macro-RAFT agent.

NMR spectrum was recorded on an Inova 400-MHz NMR instrument with $CDCl_3$ as the solvent and tetramethylsilane (TMS) as the internal standard.

Preparation of Macro-RAFT Agent

Linear poly(VBPG) (the chemical structure is shown in Scheme 1) was prepared according to the method described previously.[26] A typical procedure was as follows: VBPG (1 g, 2.759 mmol), BDB (22 mg, 0.134 mmol), AIBN (4.8 mg, 0.029 mmol), and toluene (4.5 mL) were added to a dried ampoule. The contents were purged with argon for 10 min to eliminate the dissolved oxygen. The ampoule was flame-sealed and then immersed into an oil bath at 75 °C. After 5 days, the ampoule was opened, and the contents were dissolved in THF and precipitated in 200 mL of petroleum ether three times. The obtained polymer, poly(VBPG), was dried at room temperature under vacuum until a constant weight. Poly(VBPG): $M_{n,GPC} = 6200$ g/mol, $M_w/M_n = 1.12$.

Processes of Miniemulsification and Polymerization

The recipe used in preparing the miniemulsions is listed in Table 1. The aqueous (SDS and DI water) and oil [AIBN, HD, Macro-RAFT, VBPG, and DVB (if used)] phases were first prepared separately and then mixed via magnetic stirring for 10 min in a 25-mL beaker. The mixture was followed by sonification using a Branson sonifier (model 450) at a power output setting of 800 W/L for 10 min with the beaker placed in an ice bath to absorb the excess heat produced to avoid any polymerization due to heating of the sample during the homogenization. The miniemulsion was transferred into a 15-mL round-bottom flask, degassed by purging with purity argon. The flask was then immersed into an oil bath at 75 °C. The time between miniemulsification and initiation was minimized to 5 min to reduce the droplet degradation (Ostwald ripening) period. After the desired polymerization time, the flask was opened, and the sample was demulsification by freezing in a refrigerator. For the nanoparticles prepared without crosslinker, they were washed three times with deionized water and ethanol in this order to remove SDS and HD, then dissolved in THF and precipitated in 200 mL of petroleum ether; however, for the crosslinked nanoparticles prepared in the presence of amount of crosslinker, they were washed three times with deionized water and THF in this order to remove SDS, residual monomer, toluene, and HD. The obtained polymer nanoparticles were dried at room temperature under vacuum until a constant weight.

Chiral Recognition

The chiral recognition ability of the poly(VBPG) nanoparticles was evaluated by an enantiomer-selective adsorption experiment in ethanol where a racemant was dissolved and the nanoparticles were suspended. The typical procedure was as follows: 50 mg of poly(VBPG) nanoparticles was suspended in a solution of a racemate in ethanol (concentration $= 1 \times 10^{-3}$ g/mL, volume $= 5$ mL); the mixture was stirred at room temperature overnight, then filtered, waiting for specific rotation measure to examine the ability of chiral recognition of the PVBPG nanoparticles in comparison with the original tartaric acid or mandelic acid solution. The used nanoparticles after chiral recognition were then washed with ethanol, dried for the characterization. Considering the effectiveness of reseparation, four separation–abstersion cycles were performed with various amounts of chiral nanoparticles.

RESULTS AND DISCUSSION

The Stability of Latex

Before discussing the results in detail, it is mentioned that phase separation can hardly be eliminated, no matter how to change the polymerization conditions in our experiments using BDB as RAFT agent during the RAFT miniemulsion polymerization, and that some coalescence such as floating on the surface of miniemulsion or stick to magnetic stirrer bar can easily observed. Thus, the macro-RAFT agent, poly(VBPG), was selected in this process to eliminate the secondary nucleation of new particles to suppress Ostwald ripening.[20] In this instance, the macro-RAFT agent was also served

TABLE 1 General Recipe for the RAFT Miniemulsion Polymerization of VBPG at 75 °C

	Ingredient	Content
Organic Phase (A)	VBPG	0.3 g
	Macro-RAFT agent[a]	100 mg
	HD	45 mg
	DVB	0, 3, 6, and 9 wt % based on monomer
	AIBN	0.7 mg
	Toluene	0.7 mL
Water Phase (B)	SDS	18 mg
	Deionized water	5.7 mL

[a] Poly(VBPG) : $M_{n,GPC}$ = 6200 g/mol, M_w/M_n = 1.12.

for the purpose of controlling the molecular weight and PDI of the polymer formed within the particle. Then the volume ratio of monomer to oil-solvent was on our focus. It was found that 1 g of monomer VBPG dissolved in 2–3 mL of toluene can give good performance. Visual observation and the change in droplet size as determined by HPPS and DLS were used to assess the latex stability. It was found that the latex instabilities were almost solved by reasonable combining these three important factors.

Macro-RAFT Agent-Mediated RAFT Miniemulsion Polymerization of VBPG

After solving the problem of latex instability, the kinetics of the miniemulsion polymerization of VBPG was first carried out using poly(VBPG) ($M_{n,GPC}$ = 6200 g/mol, M_w/M_n = 1.12) as the macro-RAFT agent in the absence of crosslinker DVB. The general recipe used for the miniemulsion is presented in Table 1. Figure 1 shows the kinetics of RAFT miniemulsion polymerization of VBPG. As illustrated by our experimental results, high reaction rates were obtained by monomer droplet nucleation at the first 10 h, and when the conversion exceeded 65%, the polymerization rate slowed down.

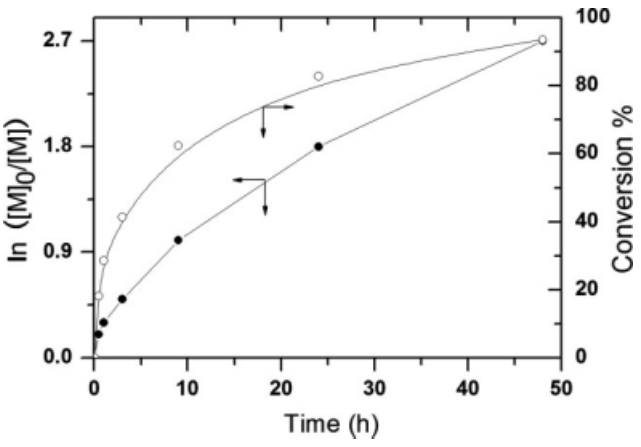

FIGURE 1 Kinetics of RAFT miniemulsion polymerization of VBPG using poly(VBPG) as the macro-RAFT agent and AIBN as the initiator. Polymerization conditions: $[VBPG]_0/[poly(VBPG)]_0/[AIBN]_0$ = 200:4:1, temperature = 75 °C; poly(VBPG) macro-RAFT agent: $M_{n,GPC}$ = 6200 g/mol, M_w/M_n = 1.12.

Figure 2 shows the evolution of the number-average molecular weight ($M_{n,GPC}$) and PDI (M_w/M_n) of poly(VBPG) on the conversion for the miniemulsion polymerization of VBPG at 75 °C. From Figure 2, it is interesting to note that the M_w/M_n values increased steadily with the evolution of conversion, and even reached 1.50 at the final conversion (93.5%). Unlike our pervious report, although the value of M_w/M_n increased with the conversion but it remained very low, never exceeded above 1.12.[26] This may be due to the fact that the superswelling could not be absolutely avoided in miniemulsion and that the difficulty of monomer transport into the latex particles from the monomer droplets through the aqueous phase leads to a disequilibrium distribution of ratios of RAFT agent to monomer within the particles. This observation was in agreement with the results reported in the literature.[29] Despite the higher M_w/M_n values in that case, the $M_{n,GPC}$ values linearly increase with the monomer conversion upto 93.5% and were good consistent with their corresponding theoretical ones, indicating that using macro-RAFT agent instead of conventional RAFT agent not only solved the problem of stability of latexes but also resulted in excellent controllability over the molecular weights of the obtained polymers in a RAFT miniemulsion polymerization system.

Effects of the Amounts of DVB on Nanoparticles

The nanoparticle size and size PDI of the obtained poly(VBPG) nanoparticle latexes were characterized by HPPS and DLS. The results are summarized in Table 2. From Table 2, it can be seen that the diameter of the poly(VBPG) nanoparticles first increased and then decreased with the increase of the amount of crosslinker in the range of 0–9 wt % and that a same changing trend was observed by both HPPS and DLS.

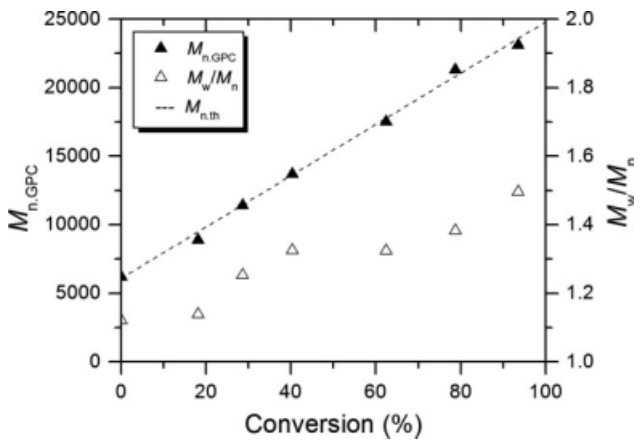

FIGURE 2 Experimental values of the number-average molecular weight ($M_{n,GPC}$) and the molecular weight distribution (M_w/M_n) as a function of conversion for the RAFT miniemulsion polymerization of VBPG using poly(VBPG) as the macro-RAFT agent and AIBN as the initiator. Polymerization conditions: $[VBPG]_0/[poly(VBPG)]_0/[AIBN]_0$ = 200:4:1, temperature = 75 °C; poly(VBPG) macro-RAFT agent: $M_{n,GPC}$ = 6200 g/mol, M_w/M_n = 1.12.

TABLE 2 Effect of the Amount of Crosslinker (DVB) on the Diameter and Size PDI of the Poly(VBPG) Nanoparticles

Amount of Crosslinker (wt %)[a]	HPPS		DLS		TEM
	D_z (nm)	Size PDI	D_z (nm)	Size PDI	D^b (nm)
0	103.9	0.108	101.0	0.188	51.3
3	126.2	0.013	119.8	0.178	130.5
6	116.9	0.098	106.4	0.146	118.0
9	104.5	0.132	100.2	0.142	65.2

[a] Based on monomer.
[b] Average diameter from the TEM images.

For 3 wt % of crosslinker, a maximum diameter (~120 nm) was obtained in that case. To further study the effect of crosslinker on the diameter and morphologies of the polymer latexes, we compared TEM images of the chiral nanoparticles prepared with crosslinker of 0, 3, 6, and 9%, as shown in Figure 3. Relative uniform and surface-smooth

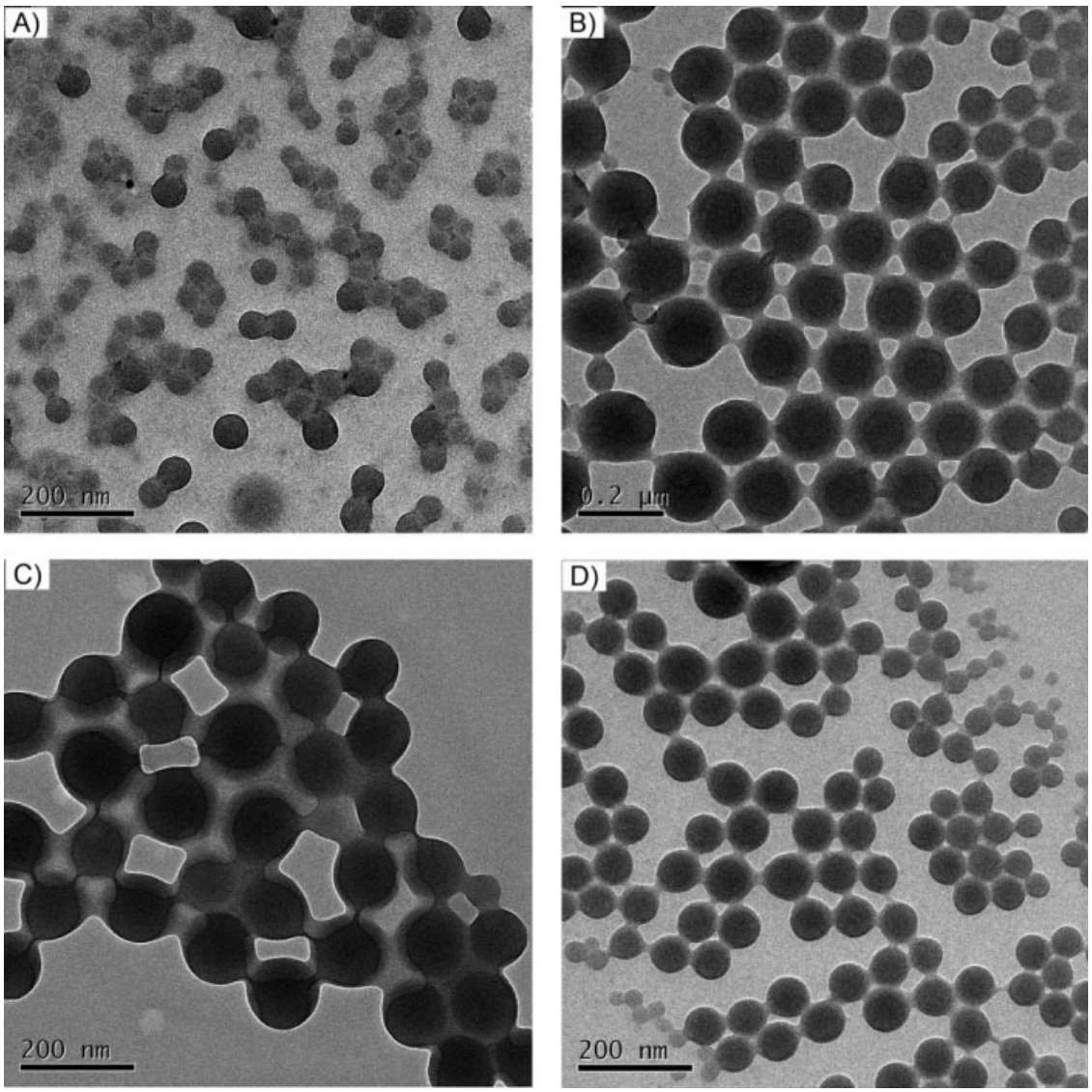

FIGURE 3 TEM images of the poly(VBPG) nanoparticle latexes of (A) without cross-linker, (B) with 3 wt % of DVB, (C) with 6 wt % of DVB, and (D) with 9 wt % of DVB. These latexes were prepared via RAFT-mediated miniemulsion polymerizations using poly(VBPG) as the macro-RAFT agent and AIBN as the initiator.

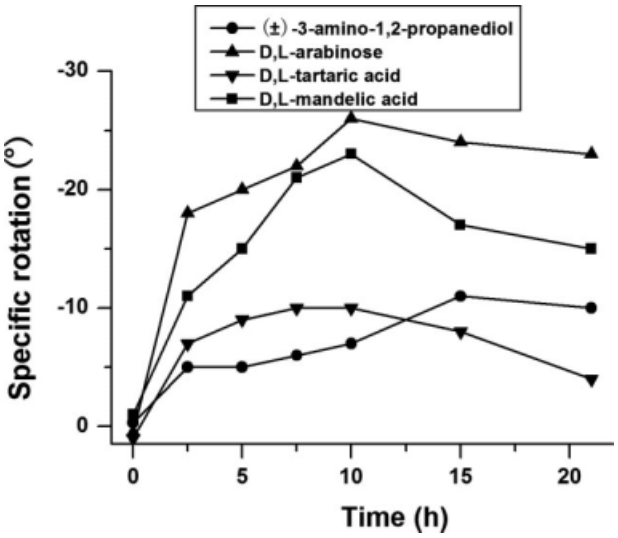

FIGURE 4 Kinetics of chiral discrimination and separation for some racemates: ±-3-amino-1,2-propanediol, D,L-arabinose, D,L-tartaric acid, and D,L-mandelic acid. Sample: crosslinked chiral nanoparticles with 3 wt % of crosslinker, 50 mg; Specific rotation: ethanol solution after chiral separation; concentration = 1 mg (racemate) /mL, volume = 5 mL; λ = 589 nm; temperature = 20 °C.

nanoparticles were observed in all cases. The diameter (D) from the TEM images was 51.3, 130.5, 118.0, and 65.2 nm for the amount of crosslinker of 0, 3, 6, and 9 wt %, respectively, which confirmed the results measured by HPPS and DLS.

Kinetics of Chiral Discrimination and Separation

To investigate the enantioselective performance of obtained chiral polymers on the different kinds of racemates, the ±-3-amino-1,2-propanediol, D,L-arabinose, D,L-tartaric acid, and D,L-mandelic acid (their chemical structures are shown in Scheme 1.) were selected for study, then a specific rotation character method was employed as reported in the literature.[26] The experiments were performed using chiral nanoparticles with 3 wt % of crosslinker at 20 °C. Under all experimental conditions, we performed time-resolved polarimeter measurements to examine potential chiral discrimination in all processes of separation. The kinetics is shown in Figure 4. From the data of Figure 4, it can be seen that the chiral nanoparticles had a good discrimination for those racemates, and the specific rotation first increases with prolonging time and then decreased a little. This phenomenon is consistent with our previous report.[26] However, when compared with the results reported previously,[26] the specific rotation both of D,L-mandelic acid and D,L-tartaric acid increased from −18° to −23° and from −9° to −10°, respectively, at the same condition, indicating better ability of chiral discrimination and separation for the chiral nanoparticles than the corresponding linear polymers. This is contributes to the fact that the crosslinked chiral nanoparticles have larger specific surface area of chiral materials and better stability in separation process due to the crosslinked structure of the obtained nanoparticles when compared with the linear chiral polymers, which can easily agglomerate during the separation process. In this study by employing the chiral nanoparticles as resolving agents, the enantioselective performance of ±-3-amino-1,2-propanediol and D,L-arabinose also show good ability of chiral discrimination during separation and a maximum specific rotation of −11° and −26° was achieved after 15 and 10 h, respectively. To assess the effectiveness of the chiral separation, the specific rotation of the corresponding "pure" substances were also measured at the same conditions, as shown in Table 3. By comparison with the results from Figure 4, it can be seen that almost complete separation was achieved for the racemates of both ±-3-amino-1,2-propanediol and D,L-tartaric acid with lower specific rotation (−14° for "pure" (S)-3-amino-1,2-propanediol and −11° for "pure" (D)-(−)-tartaric acid, respectively); however, lower effectiveness of the chiral separation was obtained for the racemates of both D,L-arabinose and D,L-mandelic acid with higher specific rotation (−86° for "pure" D-(−)-arabinose and −139° for 'pure' (D-(−)-mandelic acid, respectively) under same separation conditions.

It is noted that the chiral nanoparticles should be removed from the ethanol solution before specific rotation analysis to avoiding the interfering of chiral polymers. To ensure the full removal of the chiral polymers during analysis process, we also performed the same experiment just without any racemic material. The results of the polarimeter measurements showed no indication of the presence of chiral polymers in ethanol solution. In addition, the reason for the observed kinetic differences of chiral separation with the four kinds of racemates in Figure 4 may be contributed to the fact that all the chiral carbon contained heterochiral pairs of hydrogen though four different kinds of the racemates with different structures involved in this paper. In principle, CSP method was used in this work; therefore, intermolecular hydrogen

TABLE 3 Specific Rotations of Pure Substances[a]

Chiral Substance	Specific Rotation	Chiral Substance	Specific Rotation
(*R*)-3-Amino-1,2-propanediol	+16°	(*S*)-3-Amino-1,2-propanediol	−14°
D-(−)-Arabinose	−86°	L-(+)-Arabinose	+98°
D-(−)-Mandelic acid	−139°	L-(+)-Mandelic acid	+136°
D-(−)-Tartaric acid	−11°	L-(+)-Tartaric acid	+12°

[a] All the samples were dissolved in ethanol, concentration = 1×10^{-3} g/mL, volume = 5 mL; λ = 589 nm; temperature = 20 °C.

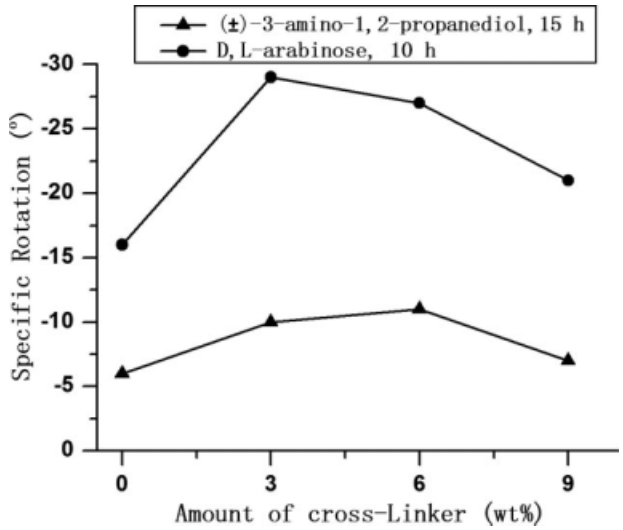

FIGURE 5 Effect of the amount of crosslinker on the chiral discrimination and separation of the obtained chiral nanoparticles. Sample: 50 mg. Specific rotation: ethanol solution after chiral separation; concentration = 1 mg (racemate) /mL, volume = 5 mL; λ = 589 nm; temperature = 20 °C; For the racemate D,L-arabinose: separations time = 10 h; For the racemate (±)-3-amino-1,2-propanediol: separation time = 15 h.

bonding interactions was the main force in the selective adsorption process for enantiomer selection. A maximum of specific optical rotation can be reached with the increase of time as shown in Figure 4; and the separation ability decreased in varying degrees when further extended hours for D,L-tartaric acid and D,L-mandelic acid. This may be due to the partial hydrolysis of hydrogen of diastereomer in acidic solution. However, for ±-3-amino-1,2-propanediol and D,L-arabinose, when prolonging the hours, the values of specific optical rotation decreased a little, indicating the separation reached a balance of maximum stability.

Effect of the Amount of Cross-Linker on Chiral Discrimination and Separation

As many articles reported that enantioselective separation mainly depends on chiral surface.[1,10–13,25,30] In consideration of finding the suitable amount of crosslinker for the separation ability of the chiral nanoparticles, we employed the obtained four chiral nanoparticles with different amount of crosslinker and two racemates D,L-arabinose and (±)-3-amino-1,2-propanediol for this study. Figure 5 shows the effect of amount of crosslinker on the chiral discrimination and separation of these nanoparticles. It can be seen that the separation abilities for the three crosslinked nanoparticles (3, 6, and 9 wt % of crosslinker) were better than the nanoparticles without crosslinking (0 wt % of crosslinker), further confirming the advantages of crosslinked nanoparticles over linear chiral polymers as mentioned above. In addition, in principle, the smaller the particle size results the greater specific surface area. The greater specific surface areas exposed, the more groups of chiral particles exposed to the surface, and the effect of separation will be better. From this point, the efficiency of the smallest crosslinked nanoparticles will have the best chiral separation ability. The specific rotation of ethanol solution for D,L-arabinose reached −29° and −27° after 10 h of separation, −10° and −11° for (±)-3-amino-1,2-propanediol after 15 h of separation, respectively, corresponding to the samples with 3 and 6 wt % of crosslinker. However, only −21° for D,L-arabinose and −7° for (±)-3-amino-1,2-propanediol were reached for the sample with 9 wt % of crosslinker although the diameter of this sample was the smallest among the three samples, as shown in Table 2. This phenomenon was contradictory with the theoretical analysis mentioned above. In fact, increasing the amount of the crosslinker will result in the increase of the density of crosslinking for the nanoparticles. When too high density of crosslinking reaches, the diffusion of the racemate molecules toward the chiral groups wrapped into the nanoparticles will become much difficult. Thus, there is a suitable amount of crosslinker for the preparation of the crosslinked nanoparticles, which may result in suitable cavities for the chiral separation. In that case, less than 6 wt % relative to chiral monomer is suitable.

Reuse of Chiral Nanoparticles

To demonstrate the repetitive ability of chiral separation of the crosslinked nanoparticles in the surface adsorption process, D,L-tartaric acid was selected as model subject for research mainly because of its biological importance and the extensive application. The specific rotation of ethanol solution after separation of D,L-tartaric acid was directly characterized by polarimeter. Briefly, 500 mg of 3% crosslinked chiral nanoparticles was suspended in a solution of 50 mL of ethanol with 50 mg of D,L-tartaric acid. The mixture was stirred for 7.5 h at 20 °C, then filtered. The solution was

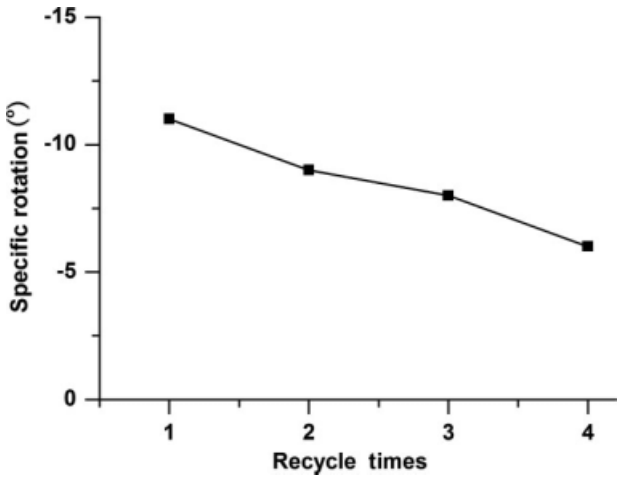

FIGURE 6 Repetitive ability of the crosslinked nanoparticles used for the chiral discrimination and separation. Sample: crosslinked chiral nanoparticles with 3 wt % of crosslinker, 500 mg. Specific rotation: ethanol solution after chiral separation, ethanol = 50 mL, D,L-tartaric acid = 50 mg, separation time = 7.5 h; λ = 589 nm; temperature = 20 °C. The chiral nanoparticles used for chiral separation washed with ethanol three times then dried before next separation.

applied to specific rotation measurement while the chiral nanoparticles were washed with ethanol three times before dried for the next use. Each time after separation, we deducted the lost nanoparticles out then suspended the remaining in a corresponding amount of ethanol dissolved D,L-tartaric acid. In this way four separation–abstersion cycles were performed. As shown in Figure 6, the nanoparticles can be reused well; however, the separation ability has somewhat loss after each cycle. This is attributable to the fact that the crosslinked nanoparticles could not disperse well in ethanol solution when dried and reused to next cycle, due to some of the agglomerations or collapsed nanoparticles was occurred while most of the nanoparticles still kept the same morphology after four times of chiral separation, which resulted in some loss of the specific area.

CONCLUSIONS

A novel way for the synthesis of well-defined chiral poly(VBPG) homopolymers and corresponding crosslinked nanoparticles with different crosslinking density, via RAFT miniemulsion polymerization using linear poly(VBPG) as the macro-RAFT agent, was demonstrated. The kinetics of RAFT miniemulsion polymerization of VBPG suggested that the polymerization proceeded in a living fashion. The amount of crosslinker had a significant effect on the size and chiral separation ability of the obtained crosslinked nanoparticles. It was found that the efficiency of chiral separation was greatly improved after transferring the crosslinked structure into the nanoparticles when compared with the chiral linear chains and that 3–6 wt % of DVB relative to the chiral monomer VBPG could give the crosslinked chiral nanoparticles better chiral separation ability for the different kinds of racemates such as D,L-arabinose and (±)-3-amino-1,2-propanediol; if continued to increase the amount of crosslinker up to 9 wt %, the ability decreased rapidly.

The financial supports of this work by the National Natural Science Foundation of China (Nos. 20874069, 50803044, 20904036, and 20974071), the Specialized Research Fund for the Doctoral Program of Higher Education contract grant (No. 200802850005), the Program of Innovative Research Team of Soochow University and the Qing Lan Project are gratefully acknowledged.

REFERENCES AND NOTES

1 Rmaile, H. H.; Schlenoff, J. B. J Am Chem Soc 2003, 125, 6602–6603.

2 Crosby, J. Tetrahedron 1991, 47, 4789–4846.

3 Diéguez, M.; Pàmies, O.; Claver, C. Chem Rev 2004, 104, 3189–3215.

4 Ward, T. J.; Baker, B. A. Anal Chem 2008, 80, 4363–4372.

5 Gübitz, G.; Schmid, M. G. Biopharm Drug Dispos 2001, 22, 291–336.

6 Hoffmann, C. V.; Pell, R.; Lämmerhofer, M.; Lindner, W. Anal Chem 2008, 80, 8780–8789.

7 Okamoto, Y. J Polym Sci Part A: Polym Chem 2009, 47, 1731–1739.

8 Ikai, T.; Okamoto, Y. Chem Rev 2009, 109, 6077–6101.

9 Yamamoto, C.; Okamoto, Y. Bull Chem Soc Jpn 2004, 77, 227–257.

10 Miyako, E.; Maruyama, T.; Kamiya, N.; Goto, M. J Am Chem Soc 2004, 126, 8622–8623.

11 Cichelli, J.; Zharov, I. J Am Chem Soc 2006, 128, 8130–8131.

12 Horvath, J. D.; Koritnik, A.; Kamakoti, P.; Sholl, D. S.; Gellman, A. J. J Am Chem Soc 2004, 126, 14988–14994.

13 Behzadi, B.; Romer, S.; Fasel, R.; Ernst, K. H. J Am Chem Soc 2004, 126, 9176–9177.

14 Sciannamea, V.; Jérôme, R.; Detrembleur, C. Chem Rev 2008, 108, 1104–1126.

15 Matyjaszewski, K.; Tsarevsky, N. V. Nat Chem 2009, 1, 276–288.

16 Moad, G.; Rizzardo, E.; Thang, S. H. Polymer 2008, 49, 1079–1131.

17 Zetterlund, P. B.; Kagawa, Y.; Okubo, M. Chem Rev 2008, 108, 3747–3794.

18 Cunningham, M. F. Prog Polym Sci 2008, 33, 365–398.

19 Luo, Y. W.; Tsavalas, J.; Schork, F. J. Macromolecules 2001, 34, 5501–5507.

20 (a) Pham, B. T. T.; Nguyen, D.; Ferguson, C. J.; Hawkett, B. S.; Serelis, A. K.; Such, C. H. Macromolecules 2003, 36, 8907–8909; (b) Lu, F. J.; Luo , Y. W.; Li, B. G. Macromol Rapid Commun 2007, 28, 868–874.

21 Al-Bagoury, M.; Buchholz, K.; Yaacoub, E. J. Polym Adv Technol 2007, 18, 313–322.

22 Lowe, A. B.; Sumerlin, B. S.; McCormick, C. L. Polymer 2003, 44, 6761–6765.

23 Okada, M. Prog Polym Sci 2001, 26, 67–104.

24 Wulff, G.; Schmid, J.; Venhoff, T. Macromol Chem Phys 1996, 197, 259–274.

25 Hazzazi, O. A.; Attard, G. A.; Wells, P. B. J Mol Catal A: Chem 2004, 216, 247–255.

26 Wang, J.; Zhu, X. L.; Cheng, Z. P.; Zhang, Z. P.; Zhu, J. J Polym Sci Part A: Polym Chem 2007, 45, 3788–3797.

27 (a) Schweitz, L.; Spégel, P.; Nilsson, S. Analyst 2000, 125, 1899–1901; (b) Spégel, P.; Schweitz, L.; Nilsson, S. Electrophoresis 2001, 22, 3833–3841.

28 (a) Quaglia, M.; De Lorenzi, E.; Sulitzky, C.; Massolini, G., Sellergren, B. Analyst 2001, 126, 1495–1498; (b) Quaglia, M.; De Lorenzi, E.; Sulitzky, C.; Caccialanza, G.; Sellergren, B. Electrophoresis 2003, 24, 952–957.

29 Zhou, X. D.; Ni, P. H.; Yu Z. Q. Polymer 2007, 48, 6262–6271.

30 Paci, I.; Szleifer, I.; Ratner, M. A. J Am Chem Soc 2007, 129, 3545–3555.